

Dephasing-enabled triplet Andreev conductance

B. Béri

Instituut-Lorentz, Universiteit Leiden, P.O. Box 9506, 2300 RA Leiden, The Netherlands
(Dated: March 2009)

We study the conductance of normal-superconducting quantum dots with strong spin-orbit scattering, coupled to a source reservoir using a single-mode spin-filtering quantum point contact. The choice of the system is guided by the aim to study triplet Andreev reflection without relying on half-metallic materials with specific interface properties. Focusing on the zero temperature, zero-bias regime, we show how dephasing due to the presence of a voltage probe enables the conductance, which vanishes in the quantum limit, to take nonzero values. Concentrating on chaotic quantum dots, we obtain the full distribution of the conductance as a function of the dephasing rate. As dephasing gradually lifts the conductance from zero, the dependence of the conductance fluctuations on the dephasing rate is nonmonotonic. This is in contrast to chaotic quantum dots in usual transport situations, where dephasing monotonically suppresses the conductance fluctuations.

PACS numbers: 74.45.+c, 85.75.-d, 73.63.Kv, 03.65.Yz

I. INTRODUCTION

The triplet superconducting proximity effect^{1,2,3} in half-metals (fully polarized ferromagnets, conducting only for one spin direction) has received a considerable attention recently, both theoretically^{4,5,6,7,8,9,10,11} and experimentally.^{12,13,14,15} The mechanism behind the effect is the process of triplet Andreev reflection at the half-metal/superconductor interface.^{2,4} The key ingredient that allows and induces this reflection process is provided by the magnetic properties of the interface between the half-metal and the superconductor: it should have a magnetization that is misaligned from that of the half-metal.^{2,4} The role of such an interface is to break all the symmetries in spin-space, thereby allowing for the spin rotations necessary for the triplet Andreev reflection. The properties of the interface, however, are not easy to manipulate in experiments, which is the reason why only a low proportion of half-metal/superconductor samples show behavior consistent with triplet Andreev reflection.^{13,14,15} Here we study triplet Andreev reflection in a setup that is free of this difficulty. The setup consists of an Andreev quantum dot¹⁶ (i.e., a quantum dot in contact with a superconductor), coupled to a normal, source reservoir via a single-mode quantum point contact (QPC), see Fig. 1. Spin-orbit scattering in the quantum dot is assumed to be strong enough that the direction of the spin is randomized in much shorter time than the typical time t_{dw} of the escape from the dot. This allows the dot to effectively play the role of the interface. The role of the half-metal is played by the QPC, which is set to the spin-selective e^2/h conductance plateau using a parallel magnetic field.¹⁷ (For simplicity, we assume that the Andreev conductance of the contact to the superconductor is much larger than e^2/h , which makes the transport properties insensitive to the details of this contact.)

A surprising feature of triplet Andreev reflection is that despite the randomized spin in the quantum dot, the conductance of such a fully phase coherent, single-channel

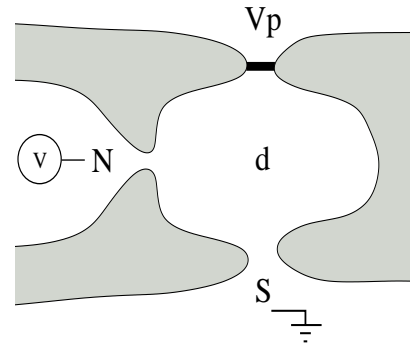


Figure 1: Sketch of the setup studied in this paper. A normal conducting chaotic quantum dot (d) coupled to a superconductor (S) via a many-mode contact, and to a normal source reservoir (N), held at an infinitesimal voltage V , via a single-mode, spin-filtering QPC. Dephasing is introduced by coupling the dot to a voltage probe (Vp) via a contact supporting N modes with a tunnel barrier (black rectangle) of transparency per mode.

system vanishes in the zero temperature, linear response regime.¹¹ While current can be passed through the system using finite voltages or temperature, it is natural to ask, whether there is still a possibility for transport in the zero temperature, linear response limit. In this paper we show that there is: relaxing the condition of full phase coherence enables the zero-bias triplet Andreev conductance to take nonzero values. In the remaining sections, our goal is to demonstrate this statement by studying the behavior of the triplet Andreev conductance in the presence of dephasing in detail.

II. VOLTAGE PROBE AS A SOURCE OF DEPHASING

We introduce dephasing by coupling the quantum dot to an additional normal reservoir, which acts as

a voltage probe.^{18,19,20,21,22} A voltage probe draws no net current, but it absorbs and reinjects quasiparticles without a phase relationship, thereby destroying phase coherence. Dephasing due to a voltage probe in normal-superconducting structures at zero temperature was studied in Refs. 23,24,25, for systems where no triplet Andreev reflection could occur. The contact to the voltage probe is characterized by the number of modes (including the spin degrees of freedom) N and the tunnel probability per mode t , which together determine the dephasing rate as $g = N t = \hbar$, where \hbar denotes the mean level spacing of the quantum dot. We consider two limits, a voltage probe with a single mode, spin-filtering contact, $N = 1$, and a voltage probe with macroscopic number of modes, $N \gg 1$. In the first case the dephasing rate is controlled by the tunnel probability. In the second case, for $g \gg 1$, which will turn out to be the regime where the conductance behaves nontrivially, the transport properties depend on N and t only through their product, i.e., the dephasing rate.²² The two limits considered here represent two types of voltage probes that appear in the context of spin-dependent quantum transport.²⁶ The probe $N = 1$ is a spin-conserving probe, while without further specification, the $N \gg 1$ can be either a spin-conserving or a spin-nonconserving voltage probe. For the system studied in this paper, there is no need for further specification, as the type of the voltage probe is unimportant due to the strong spin-orbit scattering in the quantum dot.

We formulate our problem within the framework of the scattering matrix approach. The transport quantities of interest are expressed in terms of the scattering matrix S at the Fermi energy (the chemical potential of the superconductor), relating incoming and outgoing modes (including the electron-hole degrees of freedom) in the contacts to the normal reservoirs. The currents at the contact to the source (s) and the voltage probe (v) are given by^{27,28}

$$I = \frac{e^2 X}{h} N + R^{he} - R^{ee} V \quad (1a)$$

$$R^{ij} = \text{Tr} (S^{ij})^\dagger S^{ij} \quad (1b)$$

where $i, j = s, v$, and the index e, h refers to electron and hole modes, respectively. The voltages V are measured from the chemical potential of the superconductor, which is assumed to be grounded. The voltage V is determined by demanding that no current is drawn to the voltage probe, $I = 0$. The conductance, defined by $G = V_s = I_s$ is given by

$$\frac{h}{e^2} G = 1 + R_{ss}^{he} - R_{ss}^{ee} \frac{(R_s^{he} - R_s^{ee})(R_s^{he} - R_s^{ee})}{N + R^{he} - R^{ee}} \quad (2)$$

where we substituted $N_s = 1$. Equation (2) is the starting point for our calculations. In what follows, we concentrate on systems where the motion inside the quantum dot is chaotic. We are interested in the statistics of

the conductance, which we obtain using Random Matrix Theory²⁹ for the scattering matrix S .

III. DEPHASING DUE TO A SINGLE MODE VOLTAGE PROBE

We first discuss the case voltage probe with $N = 1$. The calculational advantage of this case is that it allows for a problem with minimal dimension, with the single mode source contact and a single mode voltage probe contact resulting in a 4×4 scattering matrix. The parallel magnetic field together with the strong spin-orbit scattering places the quantum dot in the unitary symmetry class.³⁰ Consequently, the dot-superconductor system belongs to class D in the symmetry classification of Altland and Zirnbauer,³¹ which translates to $S = \tau_1 S \tau_1$ as the only constraint for the scattering matrix, besides unitarity. (τ_j denotes the j -th Pauli matrix in electron-hole space.) Assuming that the contact to the source reservoir is ideal, the two single-mode QPC-s can be characterized by the reflection matrix

$$r = \begin{pmatrix} 0 & 0 \\ 0 & 1 \end{pmatrix} P \frac{0}{1} e^{i\phi} \quad (3)$$

where the block structure reflects a grading according to the normal contacts and ϕ is the reflection phase shift for electrons at the voltage probe contact. The statistical properties of the conductance follow from the distribution of the scattering matrix, which is given by the generalization of the Poisson kernel,³²

$$P(S) / \int dS \det(1 - S^\dagger S)^3 \quad (4)$$

The probability distribution is understood with respect to the invariant measure $d(S)$ on the manifold M_D defined by $S = \tau_1 S \tau_1$ in the space of 4×4 matrices. We parametrize S as

$$S = \begin{pmatrix} e^{i\phi_1} \frac{P}{1} \frac{T}{T} \mathbb{1}_2 & e^{i\phi_2} \frac{P}{1} \frac{T}{T} \mathbb{1}_2 & W & 0 \\ e^{i\phi_2} \frac{P}{1} \frac{T}{T} \mathbb{1}_2 & e^{i\phi_1} \frac{P}{1} \frac{T}{T} \mathbb{1}_2 & 0 & W \end{pmatrix} \quad (5)$$

where $T \in \text{SU}(2)$, $\phi_1, \phi_2 \in [0, 2\pi)$, $W \in \text{SU}(2)$ and $\mathbb{1}_2 = \text{diag}(1, 1)$. (τ_j denotes the j -th Pauli matrix in spin-space.) The matrix structure in (5) corresponds to electron-hole grading. The above parametrization can be obtained from the polar decomposition introduced in the Appendix. Eq. (5) implies that $\det(S) = 1$ and that the matrix $S^{he} (S^{he})^\dagger$ has a twofold degenerate eigenvalue T . This is true for the generic setups with vanishing linear conductance in the fully phase coherent limit, i.e., if the closed Andreev quantum dot has no energy level at the Fermi energy.¹¹ (For a detailed discussion of this point we refer to the Appendix.) Using the Euler angle parametrization for W ,

$$W = \begin{pmatrix} e^{i(\phi' + \phi)/2} \cos(\phi/2) & e^{i(\phi' - \phi)/2} \sin(\phi/2) \\ e^{i(\phi' - \phi)/2} \sin(\phi/2) & e^{i(\phi' + \phi)/2} \cos(\phi/2) \end{pmatrix} \quad (6)$$

($\phi'; \phi \in [0, 2\pi) \times [0, 2\pi)$)

the invariant measure on M_D is given by $d(S)/\sin(\theta)$, and the conductance in units of e^2/h is

$$G(T; \theta) = 4 \frac{1}{T} + \frac{1}{\sin^2(\theta/2)} : \quad (7)$$

The distribution of the conductance is given by $P(G) = \int d(S) P(S) \delta(G - G(T; \theta))$, which can be reduced to

$$P(G) = \frac{3}{2G^2} \int_0^1 dx \frac{2a^2 + b^2}{x^2 (4-Gx)^2 (a^2 + b^2)^{5/2}} ;$$

$$a = 1 - (1 - \theta) \frac{1}{4-Gx} + \frac{1}{x} - 1 ; \quad (8)$$

$$\frac{b^2}{4} = (1 - \theta) - 1 \frac{1}{4-Gx} - 1 \frac{1}{x}$$

for $0 < G < 2$ and 0 otherwise. A closed form expression can be given for $\theta = 1$,

$$P_{\theta=1}(G) = 1 - \frac{2}{4-G} - \frac{G}{4} \ln \frac{G}{4-G} : \quad (9)$$

For $0 < \theta < 1$, we evaluated the integral (8) numerically. The resulting distribution is shown in the top panel of Fig. 2 for several values of θ . In the absence of dephasing, the conductance vanishes, corresponding to $P_{\theta=0}(G) = \delta(G)$. With the gradual introduction of dephasing, G is enabled to take nonzero values, leading to a widening of the conductance distribution with increasing dephasing rate, eventually reaching the distribution (9) for $\theta = 1$. In the bottom panel of Fig. 2 we show the dependence of the average and the variance of the conductance on θ . While the average conductance increases monotonically with increasing dephasing rate, the variance increases to a maximum at $\theta \approx 0.8$, which is followed by a slight decrease. The finite value of the conductance fluctuations at $\theta = 1$ (corresponding to the maximal dephasing for $N = 1$) indicates that a single channel voltage probe can not lead to a complete loss of phase coherence (as we will see below, without phase coherence, the conductance fluctuations are suppressed back to zero). For weak dephasing, $\theta \ll 1$, the conductance distribution is rapidly decaying away from $G = 0$ and it has the scaling form $P(G) = f(G/\theta) = G$. This results in the dependence

$$hG^n \propto \theta^{-n}; \quad n \geq 1 \quad (10)$$

for the n -th moment of the conductance.

IV. DEPHASING DUE TO A MULTIMODE VOLTAGE PROBE

Now we turn to the case of the voltage probe with macroscopic number of channels, $N \gg 1$. While it might

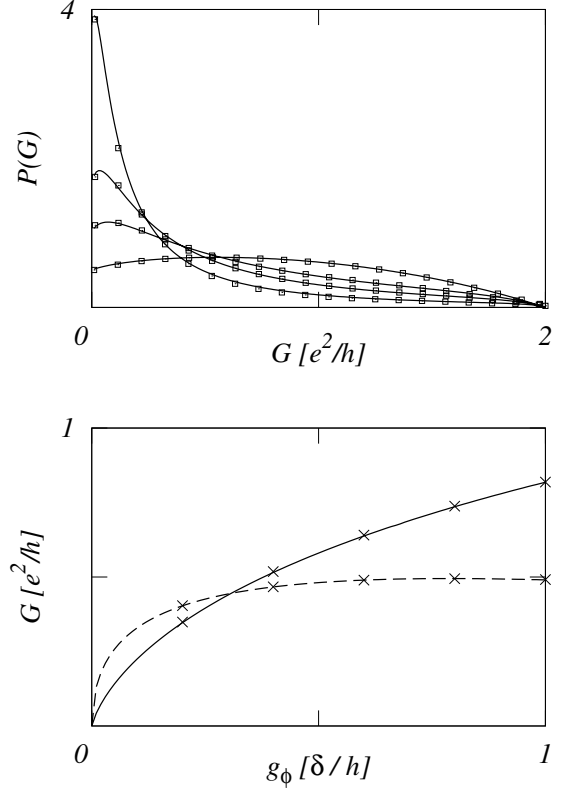


Figure 2: Upper panel: Probability distribution [Eq. (8)] of the conductance for $N = 1$, for various values of the dephasing rate $g = \hbar/\tau$. The curves, in order of decreasing maximum, correspond to $\theta = 0.2, 0.4, 0.6, 1$, respectively. The empty squares represent smoothed histograms obtained from 3000 numerically generated scattering matrices for each value of θ , for a system where the superconducting contact supports 50 propagating modes. Lower panel: the average (solid line) and the standard deviation (dashed line) of the conductance as a function of g . The crosses are results of the numerical simulation.

be possible to make some analytical progress using the Poisson kernel distribution of Ref. 32 and following similar steps to the calculation of Ref. 22, we resort to a simpler approach and obtain the statistics of the conductance by generating an ensemble of scattering matrices numerically. The scattering matrix S is expressed in terms of the electron scattering matrix

$$S_N = \begin{pmatrix} r & t^0 \\ t & r^0 \end{pmatrix} \quad (11)$$

of the normal region. Here r describes reflection from the dot through the normal contacts, r^0 describes reflection through the superconducting contacts, t corresponds to transmission to the superconducting, and t^0 to the normal contacts. The necessary blocks of S in electron-hole

grading are given by^{29,33}

$$S^{ee} = r \ell_2 r_2^0 (1 + r_2^0 r_2^0)^{-1} t; \quad (12a)$$

$$S^{he} = \ell_2 (1 + r_2^0 r_2^0)^{-1} t; \quad (12b)$$

The scattering matrix S_N can be expressed using the statistical mapping^{34,35}

$$S_N = \frac{P}{1} - \frac{P}{1} \frac{1}{S_0} \frac{P}{1} = S_0; \quad (13)$$

where S_0 is unitary and is a diagonal matrix containing the transmission probabilities of the contacts with $s_{11} = 1$ corresponding to perfect transmission through the single mode QPC and $s_{jj} = 1$ for $1 < j \leq N + 1$ describing tunneling at the voltage probe. We took $s_{jj} = 1$ for $j > N + 1$, corresponding to the contact to the superconductor. The results do not depend on this choice, as long as the Andreev conductance of the contact is much greater than e^2/h . Using the mapping (13), the distribution of S_N is obtained by taking S_0 from the circular unitary ensemble,^{34,35} which we generated numerically.³⁶ For a mutual test of the program and the calculations, we first show results for $N = 1$ in Fig. 2. As it is seen, the agreement between the calculation and the numerics is perfect. The conductance distribution in the limit $N \rightarrow 1$ is shown in the top panel of Fig. 3 for several values of the dephasing rate g . The distribution $P_g(G)$ initially widens from $P_{g=0} = \delta(G)$ with increasing g and then it gradually narrows again to $P_{g=1} = \delta(G - G_{\text{class}})$, where

$$G_{\text{class}} = \frac{1}{G_{\text{QPC}}} + \frac{1}{G_{\text{NS}}} \quad G_{\text{QPC}} = 1 \quad (14)$$

is conductance of the single mode QPC and the Andreev conductance of the superconducting contact in series, in units of e^2/h . The dependence of the average and the variance of the conductance on g is shown in bottom panel of Fig. 3. While the average conductance increases monotonically to its classical value, the conductance fluctuations display nonmonotonic behavior, corresponding to the initial widening and the final re-narrowing of the conductance distribution. Fig. 3 also shows a comparison between the limits $N \rightarrow 1$ and $N \rightarrow \infty$. For a given value of g , the conductance distribution close to $G = 0$ is suppressed for $N \rightarrow \infty$, in contrast to the single channel case, where $P(G = 0)$ is finite. The average conductance increases faster for $N \rightarrow \infty$ towards its classical value, while the conductance fluctuations are suppressed compared to $N \rightarrow 1$.

V. CONCLUSIONS

In summary, we have studied in detail how dephasing due to a voltage probe enables a nonzero value for the zero temperature, zero-bias triplet Andreev conductance in Andreev quantum dots with a single-channel

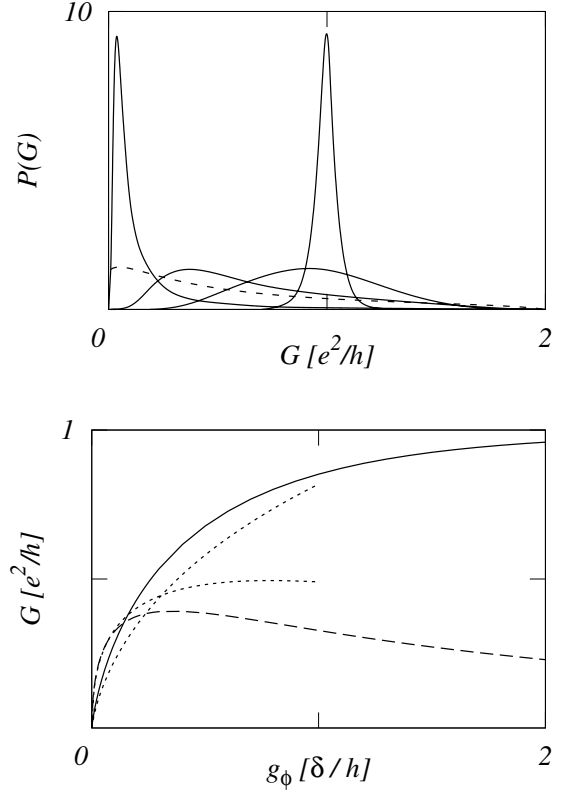


Figure 3: Upper panel: Probability distribution of the conductance for $N = 1$, for different values of the dephasing rate g . The solid curves, in order of increasing position G of the maximum, correspond to $g/h = 0.05, 0.5, 1.5, 10$, respectively. The curves are obtained by smoothing histograms from 3000 numerically generated scattering matrices for each value of g , with $N = 100$, for a system where the superconducting contact supports 50 propagating modes. For comparison, we show the distribution for $N = 1$, $g/h = 0.5$ (dashed line). Lower panel: the average (solid line) and the standard deviation (dashed line) of the conductance as a function of g . For comparison, the dotted lines show the corresponding functions for $N = \infty$.

spin-filtering source point contact. We focused on systems where the quantum dot is chaotic, and obtained the full distribution of the conductance as a function of the dephasing rate for two limiting cases for the number of modes N in the voltage probe contact, $N = 1$, and $N \rightarrow \infty$. Compared to chaotic quantum dots in other transport situations, our findings for the conductance are quite unusual. Dephasing is known to monotonically suppress the conductance fluctuations, in general.^{21,29,37,38} In contrast, as dephasing gradually enables transport, the fluctuations of the triplet Andreev conductance are initially enhanced, which is followed by a suppression for strong dephasing, i.e., the overall dependence on the dephasing rate is nonmonotonic.

It is worthwhile to point out that in the $N \rightarrow \infty$ case,

unlike Ref. 37, we did not intend to use the voltage probe to model dephasing processes intrinsic to the quantum dot, since accounting for the temperature dependence of such processes would necessitate considering the effect of thermal smearing.³⁸ Instead, our results apply to the situation where the dephasing rate is controlled by a real, physically present voltage probe. Experimental control of the dephasing rate using a voltage probe was demonstrated very recently in the work of Rouleau et al.³⁹ This makes us believe that, in principle, it is realistic to test our predictions in experiments.

Acknowledgments

This work originated from discussions with P. W. Brouwer. The author has also benefited from discussions with C. W. J. Beenakker. This research was supported by the Dutch Science Foundation NWO/FOM.

Appendix A: ELECTRON-HOLE SYMMETRY, POLAR DECOMPOSITION AND ANDREEV REFLECTION EIGENVALUES

The Andreev reflection eigenvalues T_j are the eigenvalues of the matrix $S^{he}(S^{he})^y$. We prove here the consequences of electron-hole symmetry on these quantities, and relate them to the condition of the absence of energy level of the closed Andreev quantum dot at the Fermi energy.

Theorem: At the Fermi energy, the degeneracy d_j of the Andreev reflection eigenvalue T_j is even if $T_j(1 - T_j) \neq 0$, and $\det(S) = (-1)^{d_u}$, where d_u is the degeneracy of the unit Andreev reflection eigenvalue, if present, $d_u = 0$ otherwise. Furthermore, the scattering matrix at the Fermi energy can be decomposed in electron-hole grading as

$$S = \begin{pmatrix} U & 0 & \hat{R} & \hat{T} & V & 0 \\ 0 & U & \hat{T} & \hat{R} & 0 & V \end{pmatrix}; \quad (\text{A } 1)$$

where U and V are unitary matrices,

$$\hat{R} = \bigoplus_j^M \frac{p}{1 - T_j} \mathbb{1}_{d_j} \quad (\text{A } 2a)$$

$$\hat{T} = \bigoplus_j^M \frac{p}{T_j} \mathbb{1}_{d_j}; \quad (\text{A } 2b)$$

and $\hat{\Lambda} = \bigoplus_j^L \Lambda_j$, where

$$\Lambda_j = \begin{cases} \mathbb{1}_{d_j} & \text{if } T_j(1 - T_j) = 0 \\ \mathbb{1}_{d_j=2} & \text{otherwise.} \end{cases} \quad (\text{A } 3)$$

Proof: Following from the electron-hole symmetry $S = -S^y$, the scattering matrix has the block decomposition

$$S = \begin{pmatrix} S^{ee} & S^{he} \\ S^{he} & S^{ee} \end{pmatrix}; \quad (\text{A } 4)$$

We start with the singular value decomposition

$$S^{ee} = U^0 \hat{R} V^0; \quad (\text{A } 5)$$

where U^0, V^0 are unitary matrices. Using $(S^y S)^{ee} = \mathbb{1}$ and $(S S^y)^{ee} = \mathbb{1}$, one finds that

$$S^{he} = U^0 Z \hat{T} V^0; \quad (\text{A } 6)$$

Here Z is a block diagonal unitary matrix,

$$Z = \bigoplus_j^M Z_j; \quad \dim Z_j = d_j; \quad (\text{A } 7)$$

Substituting (A 5) and (A 6) into $(S^y S)^{he} = 0$ leads to

$$q \frac{1}{T_j(1 - T_j)} Z_j = q \frac{1}{T_j(1 - T_j)} Z_j^T \quad (\text{A } 8)$$

For $T_j(1 - T_j) \neq 0$, Z_j is antisymmetric, and due to its unitarity $\det(Z_j) \neq 0$, from which it follows that d_j is even. Being antisymmetric and unitary, Z_j can be decomposed as^{40,41}

$$Z_j = U_j^T \hat{\Lambda}_j U_j; \quad \hat{\Lambda}_j = \mathbb{1}_{d_j=2}; \quad (\text{A } 9)$$

where U_j is unitary. For $T_j = 0; 1$, Eqn. (A 8) is automatically satisfied, without further requirements for Z_j . For the zero Andreev reflection eigenvalue, if present, we can set $Z_j = U_j^T U_j$ with an arbitrary unitary matrix U_j , as for $T_j = 0$, Z_j drops out from (A 6). For the unit Andreev reflection eigenvalue, if present, we write $Z_j = U_j^T U_j^0$ with U_j, U_j^0 unitary. Taken together, the matrix Z can be written as

$$Z = \bigoplus_j^M U_j^T U_j^0; \quad (\text{A } 10)$$

where $U_j^0 = U_j$ for $T_j \neq 1$. Writing U^0 and V^0 as

$$U^0 = U \bigoplus_j^M U_j A_j \quad (\text{A } 11a)$$

$$V^0 = \bigoplus_j^M U_j^0 A_j V; \quad (\text{A } 11b)$$

with U, V unitary, one finds

$$S^{ee} = U \hat{R} V \quad (\text{A } 12a)$$

$$S^{he} = U \hat{T} V; \quad (\text{A } 12b)$$

which gives the decomposition (A 1) upon substitution in Eq. (A 4). The decomposition (A 1) satisfies the unitarity and electron-hole symmetry requirements, therefore

there are no further relations between the matrices U and V . The result $\det(S) = (-1)^{j_0}$ follows straightforwardly.

Note that in Eq. (5), we assumed $\det(S) = 1$, however only $\det(S) = \pm 1$ follows from $S = \pm S^{-1}$. We show below that this is a valid assumption in the generic situation that there is no energy level of the closed Andreev quantum dot at the Fermi energy. Using the channel coupled model employed in Ref. 31, the scattering matrix can be expressed as²⁹

$$S_E = \frac{1 + iH_E}{1 - iH_E} : \quad (\text{A } 13)$$

Here the Hermitian matrix $H_E = \pm H_E^{-1}$ is a projection of $(H - E)^{-1}$, where H models the closed Andreev quantum dot. If H has no zero eigenvalues, i.e., there is no level at the Fermi energy, the matrix H_E can be taken at $E = 0$ without complications. Follow-

ing from the symmetry of $H_{E=0}$, the eigenvalues of S come in complex conjugate pairs, therefore, $\det(S) = \pm 1$. (If there is a level at the Fermi energy, an eigenvalue of H_E can diverge as $E \rightarrow 0$ while another can tend to zero, leading to a $(1; -1)$ eigenvalue pair of S , and thereby to $\det(S) = -1$.) This result, together with $\det(S) = (-1)^{j_0}$, contains as a special case the finding of Ref. 11, that for a single mode system, $S^{\text{he}} = 0$ at the Fermi level, if the closed Andreev quantum dot has no level at the Fermi energy. Indeed, for such a system, S is a 2×2 matrix, i.e., there is a single Andreev reflection eigenvalue. As it is singly degenerate, it can be only zero or unity, and $\det(S) = 1$ guarantees that it is zero. For the 4×4 matrix in Eq. 5), the degeneracy of the Andreev reflection eigenvalue also follows from $\det(S) = 1$. If there was no degeneracy, the eigenvalues could be only a zero and a unit eigenvalue. This would mean $\det(S) = -1$.

-
- ¹ F. S. Bergeret, A. F. Volkov, and K. B. Efetov, Phys. Rev. Lett. 86, 4096 (2001).
 - ² A. K. Adigrobov, R. I. Shekhter, and M. Jonson, Europhys. Lett. 54, 394 (2001).
 - ³ F. S. Bergeret, A. F. Volkov, and K. B. Efetov, Rev. Mod. Phys. 77, 1321 (2005).
 - ⁴ M. Eschrig, J. Kopp, J. Cuevas, and G. Schon, Phys. Rev. Lett. 90, 137003 (2003).
 - ⁵ V. Braude and Y. V. Nazarov, Phys. Rev. Lett. 98, 077003 (2007).
 - ⁶ Y. A. Sano, Y. Tanaka, and A. A. Golubov, Phys. Rev. Lett. 98, 107002 (2007).
 - ⁷ Y. A. Sano, Y. Sawa, Y. Tanaka, and A. A. Golubov, Phys. Rev. B 76, 224525 (2007).
 - ⁸ S. Takahashi, S. Hikino, M. Mori, J. Martinek, and S. Maekawa, Physical Review Letters 99, 057003 (2007).
 - ⁹ M. Eschrig and T. Lofwander, Nature Physics 4, 138 (2008).
 - ¹⁰ A. V. Galaktionov, M. S. Kalenkov, and A. D. Zaikin, Phys. Rev. B 77, 094520 (2008).
 - ¹¹ B. Beri, J. N. Kupferschmidt, C. W. J. Beenakker, and P. W. Brouwer, Phys. Rev. B 79, 024517 (2009).
 - ¹² R. S. Keizer, S. T. Goennenwein, T. M. Klapwijk, G. Miao, G. Xiao, and A. Gupta, Nature 439, 825 (2006).
 - ¹³ V. N. Krivoruchko, V. Y. Tarenkov, A. I. Dyachenko, and V. N. Varyukhin, Europhys. Lett. 75, 294 (2006).
 - ¹⁴ K. A. Yates, W. R. Branford, F. Magnus, Y. Miyoshi, B. Morris, L. F. Cohen, P. M. Sousa, O. Conde, and A. J. Silvestre, Appl. Phys. Lett. 91, 172504 (2007).
 - ¹⁵ V. N. Krivoruchko and V. Y. Tarenkov, Phys. Rev. B 75, 214508 (2007).
 - ¹⁶ C. W. J. Beenakker, Lect. Notes Phys. 667, 131 (2005).
 - ¹⁷ R. M. Potok, J. A. Folk, C. M. Marcus, and V. Umansky, Phys. Rev. Lett. 89, 266602 (2002).
 - ¹⁸ M. Buttiker, Phys. Rev. B 33, 3020 (1986).
 - ¹⁹ M. Buttiker, IBM J. Res. Dev. 32, 63 (1988).
 - ²⁰ C. M. Marcus, R. M. Westervelt, P. F. Hopkins, and A. C. Gossard, Phys. Rev. B 48, 2460 (1993).
 - ²¹ H. U. Baranger and P. A. Mello, Phys. Rev. B 51, 4703 (1995).
 - ²² P. W. Brouwer and C. W. J. Beenakker, Phys. Rev. B 55, 4695 (1997).
 - ²³ N. Mortensen, A. Jauho, and K. Flensberg, Superlatt. Microstruct. 28, 67 (2000).
 - ²⁴ T. Gramsch and M. Buttiker, Phys. Rev. B 61, 8125 (2000).
 - ²⁵ M. Belogolovskii, Phys. Rev. B 67, 100503 (2003).
 - ²⁶ C. W. J. Beenakker, Phys. Rev. B 73, 201304 (2006).
 - ²⁷ Y. Takane and H. Ebisawa, J. Phys. Soc. Jpn. 61, 1685 (1992).
 - ²⁸ C. J. Lambert, V. C. Hui, and S. J. Robinson, J. Phys.: Condens. Matter 5, 4187 (1993).
 - ²⁹ C. W. J. Beenakker, Rev. Mod. Phys. 69, 731 (1997).
 - ³⁰ I. L. Aleiner and V. I. Fal'ko, Phys. Rev. Lett. 87, 256801 (2001), 89, 079902 (E) (2002).
 - ³¹ A. A. Kland and M. R. Zimbauer, Phys. Rev. B 55, 1142 (1997).
 - ³² B. Beri, arXiv:0902.2164 (2009).
 - ³³ C. W. J. Beenakker, Phys. Rev. B 46, 12841 (1992).
 - ³⁴ P. A. Mello, P. Pereyra, and T. Seligman, Ann. Phys. 161, 254 (1985).
 - ³⁵ P. W. Brouwer, Phys. Rev. B 51, 16878 (1995).
 - ³⁶ F. Mezzadri, Notices-AMS 54, 592 (May, 2007).
 - ³⁷ P. W. Brouwer and C. W. J. Beenakker, Phys. Rev. B 51, 7739 (1995).
 - ³⁸ A. G. Huibers, S. R. Patel, C. M. Marcus, P. W. Brouwer, C. I. Duinoz, and J. S. Harris, Phys. Rev. Lett. 81, 1917 (1998).
 - ³⁹ P. Rouleau, F. Portier, P. Roche, A. Cavanna, G. Faini, U. Gennser, and D. Mailly, arXiv:0903.0491 (2009).
 - ⁴⁰ D. C. Youla, Canad. J. Math 13, 694 (1961).
 - ⁴¹ J. Schliemann, J. I. Cirac, M. Kus, M. Lewenstein, and D. Loss, Phys. Rev. A 64, 022303 (2001).